

# Impact of the Temperature Dependency of Fiberglass Insulation R-Value on Cooling Energy Use in Buildings

Ronnen Levinson, Hashem Akbari, and Lisa M. Gartland, Ernest Orlando Lawrence Berkeley National Laboratory

Building energy models usually employ a constant, room-temperature-measured value for the thermal resistance of fiberglass roof insulation. In summer, however, the mean temperature of roof insulation can rise significantly above room temperature, lowering the insulation's thermal resistance by 10% to 20%. Though the temperature dependence of the thermal resistance of porous materials like fiberglass has been extensively studied, it is difficult to theoretically predict the variation with temperature of a particular fiberglass blanket, from first principles. Heat transfer within fiberglass is complicated by the presence of three significant mechanisms—conduction through air, conduction through the glass matrix, and radiative exchange within the matrix—and a complex, unknown internal geometry. Purely theoretical models of fiberglass heat transfer assume highly simplified matrix structures and require typically-unavailable information about the fiberglass, such as its optical properties. There is also a dearth of useful experimental data. While the thermal resistances of many individual fiberglass samples have been measured, there is only one practical published table of thermal resistance vs. both temperature and density. Data from this table was incorporated in the DOE-2 building energy model. DOE-2 was used to simulate the roof surface temperature, roof heat flux, and cooling energy consumption of a school bungalow whose temperature and energy use had been monitored in 1992. The DOE-2 predictions made with and without temperature variation of thermal conductivity were compared to measured values. Simulations were also run for a typical office building. Annual cooling energy loads and annual peak hourly cooling powers were calculated for the office building using both fixed and variable thermal conductivities, and using five different climates. The decrease in the R-value of the office building's roof led to a 2% to 4% increase in annual cooling energy load.

## INTRODUCTION

Models of building energy use generally employ a constant R-value to describe the thermal resistance of roof insulation. In practice, however, the thermal resistance of a fiberglass blanket underneath a hot roof can fall significantly below its nominal room-temperature value because the effective thermal conductivity of fiberglass changes with temperature. This paper will review theories and experimental data describing the temperature dependence of the effective thermal conductivity of fiberglass, then present simulations of building energy use that quantify the extent to which a decline in R-value increases roof heat flows and cooling energy loads.

### Literature Review

An immense body of literature addresses heat transfer in porous media like fiberglass. For our purposes, it may be divided into

- (1) efforts to theoretically predict the heat flux from first principles, or approximations thereof;
- (2) elementary theoretical overviews;
- (3) measurements of effective thermal conductivity vs. temperature made for specific materials; and
- (4) compilations of measurements of effective thermal conductivity vs. temperature and density that cover a range of materials.

**First Principles.** Numerous texts and journal articles model apply first principles of radiative heat transfer to simple geometries, e.g. packed spheres or parallel cylinders, which have been chosen as tractable idealizations of the complex internal geometries of porous media (Kaviany 1991). Others employ two-flux or linear anisotropic scattering approximations to simplify the equation of transfer of radiation intensity (Tong & Tien 1983). A solution from first principles requires the spectral absorption and scattering coefficients of the medium, along with its scattering phase function; these in turn depend on the material properties and geometry of the fibers and their binder. Tong's approximate treatment requires only the complex reflective index, size distribution, and volume fraction of the fibers, but he found only qualitative agreement between his theory and measured results. Moreover, none of these parameters is actually known for an arbitrary sample of fiberglass characterized only by its thickness and R-value. Pore length scale, for

example, is independent of porosity, and Kaviani reports a strong variation with pore size of the effective thermal conductivity of a medium of fixed porosity (Kaviani 1991, 132).

Conduction heat transfer in porous media is also well-represented in the literature. One review (Progelhof, Throne & Reutsch 1976) lists 24 models of the combined thermal conductivity of the solid and gas components of a porous medium, of which the three simplest models—serial, parallel, and geometric mean—require knowledge of only the porosity and the thermal conductivities of the solid and gas components. More sophisticated, less applicable models assume specific geometries, known pore sizes, etc.

**Overviews.** Texts on heat transfer (Gebhart 1993, 436-51) or thermal conductivity (Pratt 1969) often include a section on insulation that discusses the elementary theory of heat transfer in porous media to roughly the level of detail given in the theory section of this paper.

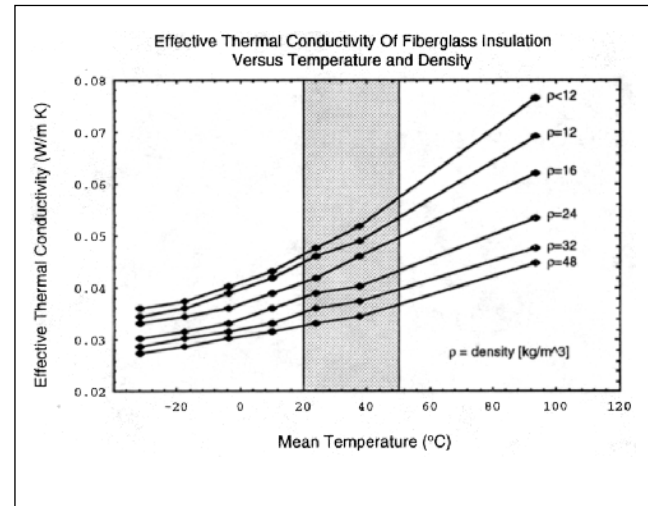
**Measurements.** Researchers have published the measured temperature variation of the effective thermal conductivity of particular specimens of fiberglass mats, usually fitting it to a two-term polynomial with a radiative term proportional to  $T^3$  and a  $T^n$ , conductive term proportional to  $T^n$ ,  $n$  between  $\frac{1}{2}$  and  $\frac{3}{2}$ . Temperatures ranges are usually for either cryogenic uses ( $-263^\circ$  to  $127^\circ$  C) or high-temperature applications ( $27^\circ$  to  $427^\circ$  C); studies with resolution better than  $50^\circ$  C in the range of hot attic temperatures ( $20^\circ$  to  $70^\circ$  C) appear to be rare. Moreover, these studies look at fiberglass mats, which can be ten times denser than blankets (Cabannes et al. 1979).

**Compilations.** Several handbooks tabulate the effective thermal conductivity of fiberglass at various densities and temperatures. One lists the conductivity of more than 60 different insulators of assorted densities at  $100^\circ$  F intervals over various temperature ranges (Turner & Malloy 1981). Another study collected data on fiberglass thermal conductivity at many densities, but at only two well-spaced temperatures,  $24^\circ$  C and  $249^\circ$  C (Wilkes 1981). The American Society of Heating, Refrigerating, and Air-conditioning Engineers (ASHRAE) Fundamentals Handbook (ASHRAE 1985, 23.17) provides a very practical table of conductivity for temperatures ranging from  $-32^\circ$  to  $94^\circ$  C at intervals of  $14^\circ$  C, and for densities ranging from 12 to  $48 \text{ kg m}^{-3}$  (Figure 1). The ASHRAE data is often cited in other books, but ASHRAE does not list its own sources.

## Theory

The temperature dependence of the R-value of fiberglass insulation may be sought theoretically, from first principles,

**Figure 1.** Effective Thermal Conductivity of Fiberglass vs. Temperature and Density



Source: Based on ASHRAE (1985) 23.17.

Note: The effective thermal conductivity of fiberglass, plotted vs. temperature at several densities. The mean temperature of insulation in a hot attic usually lies inside the shaded temperature range.

or empirically, by fitting an expression for  $k_e(T)$  to the ASHRAE data.

**First Principles.** A fiberglass blanket may be idealized as a one-dimensional, homogeneous, porous slab of finite thickness designed to trap air within a matrix of glass fibers. Vibrational conduction through the glass and air, combined with absorption and re-emission of thermal radiation through the glass matrix, transfer heat from the warm to the cool side of the blanket. Natural convection may also be present in low-density fiberglass.

Conduction through a one-dimensional medium is predicted by Fourier's law,

$$q = -k \frac{dT}{dx},$$

where  $q$  is the heat flux per unit area,  $k$  is the thermal conductivity, and  $dT/dx$  is the local temperature gradient. In the temperature range of interest to attics in summer, the thermal conductivity of air is about 100 times smaller than that of glass, and increases about 8% as the temperature rises from  $20^\circ$  to  $50^\circ$  C (White 1988, 682). The thermal conductivity of glass rises or falls about 3% over this temperature range, depending on the type of glass (White 1988, 675). Since fiberglass is typically 90% air by volume, thermal conduction along the glass fibers would be about 10 times greater than that through the still air if the glass and air conducted heat in parallel.

Many models have been proposed to determine a thermal conductivity that combines conduction through air with that through the glass. The three simplest are the parallel resistance model,

$$k_{par} = \phi k_a + (1 - \phi) k_g;$$

the serial resistance model,

$$1/k_{ser} = \phi/k_a + (1 - \phi)/k_g;$$

and the geometric mean model,

$$k_{mean} = k_{ser}^n k_{par}^{(1-n)},$$

where  $\phi$  is the porosity (void fraction) of the fiberglass matrix,  $k_a$  is the thermal conductivity of air,  $k_g$  is the thermal conductivity of glass, and  $n$  is an empirical constant. Predicting the actual combined thermal conductivity  $k_c$  is difficult for a complex geometry, and even more so for an unknown, complex geometry, but its value should be bounded between the minimum, serial conductivity and the maximum, parallel conductivity.

Natural convection of air is found in low-density fibrous insulations (less than  $16 \text{ kg m}^{-3}$ ) and vanishes in high-density insulations (greater than  $39 \text{ kg m}^{-3}$ ) (Powell, Krarti & Tuluca 1989). The free convection coefficient  $k_f$  varies slowly with temperature, and is typically proportional to the fourth root of the difference between surface and air temperature,  $(T_{surface} - T_{air})^{1/4}$  (White, 405). We may neglect its temperature dependency and write  $k_f = k_f(\rho)$ , where  $\rho$  is density.

If a fiberglass blanket is optically thick to thermal radiation—meaning that a photon of thermal radiation is likely to be absorbed as it traverses the fiberglass—the radiative heat transfer through the blanket is predicted by the Rosseland diffusion approximation,

$$q = -k_r \frac{dT}{dx},$$

where

$$k_r = c_r T^3$$

and  $c_r$  is a constant that depends on both the glass fiber geometry and the electromagnetic properties of the glass (Brewster 1992, 385–86). A typical six-inch thick, 90% porous fiberglass blanket should be optically thick to thermal radiation because it presents a path at least 30 times longer than the typical distance that a thermal radiation photon can travel before being absorbed in glass. However, the glass

fiber geometry and detailed electromagnetic properties of the glass are generally unavailable. Thus the constant  $c_r$  is unknown, and we can say only that

$$q_r \propto T^3 \frac{dT}{dx},$$

The total heat flux across the blanket is

$$q = -k_e \frac{dT}{dx},$$

where the effective thermal conductivity  $k_e$  is given by

$$k_e = k_r + k_c + k_f,$$

$$k_r = c_r T^3,$$

$$k_c = k_{ser}^n k_{par}^{(1-n)},$$

$$k_f = k_f(\rho),$$

$$1/k_{ser} = \phi/k_a + (1 - \phi)/k_g,$$

$$k_{par} = \phi k_a + (1 - \phi) k_g,$$

$$k_g(T) = c_{1_g} + c_{2_g} T,$$

$$k_a(T) = c_{1_a} + c_{2_a} T.$$

Simple linear approximations may be employed for the thermal conductivities of glass and air over the temperature of interest.

The thermal resistance  $R$  is just the ratio of the blanket thickness  $l$  to the effective thermal conductivity  $k_e$ . However, the radiation coefficient  $c_r$ , geometric-mean-law constant  $n$ , porosity  $\phi$ , and glass conductivity constants  $c_{1_g}$  and  $c_{2_g}$  are generally unknown for a fiberglass blanket that is characterized only by its thickness and nominal R-value. The internal free convection coefficient  $k_f$  is also unknown and may be significant for low-density blankets. Thus it is quite difficult to predict  $k_e(T)$  from first principles for an arbitrary specimen of fiberglass.

**Empirical Curve Fitting.** The nominal R-value of a sample of insulation,  $R_{nom}$ , is its thermal resistance measured at nominal room temperature  $T_{room} = 21^\circ \text{C}$ . The ASHRAE data can be used to predict the temperature variation of a particular sample of fiberglass by first calculating the sample's nominal effective thermal conductivity  $k_{nom} = l/R_{nom}$ , then selecting the curve of  $k_e(T)$  in Figure 1 for which  $k_e(T_{room}) = k_{nom}$ .  $k_e(T)$  curves may also be interpolated for densities between those plotted in Figure 1.

The ASHRAE data for  $k_e(T)$  for a given density can easily be fit with any second-or-higher degree, two-or-more term polynomial of the form

$$k_e(T) = a T^n + b T^m;$$

it does not really matter whether  $m$  and  $n$  relate to physical phenomena such as gas conduction or radiative heat transfer. The drawback to using the ASHRAE data is that its sources are not cited.

Given the difficulty of predicting the effective thermal conductivity of fiberglass from theory, it would be helpful if manufacturers or research laboratories measured and labeled the R-value of insulations over the range of mean temperatures to which they are subject in building applications, say  $-20^\circ$  to  $50^\circ$  C.

## Simulations

In summer, the surface temperature of a dark roof can reach  $80^\circ\text{C}$ , raising the mean temperature of roof insulation sandwiched between the  $80^\circ\text{C}$  roof and a  $21^\circ\text{C}$  air-conditioned room to approximately  $50^\circ\text{C}$ . ASHRAE data indicate that the effective thermal conductivity of fiberglass insulation at a mean temperature of  $50^\circ\text{C}$  is 10% to 20% higher than at room temperature. Low-density fiberglass shows the greatest variation of effective thermal conductivity with temperature, and high-density fiberglass the least (Figure 1). Since heat flow is proportional to the effective thermal conductivity, we expect a 10–20% increase in heat flow through the roof as the insulation's mean temperature increases from  $21^\circ\text{C}$  to  $50^\circ\text{C}$ . We would also expect an air-conditioned building with a hot roof, and thus hot insulation, to consume more cooling energy than predicted from the insulation's nominal R-value. However, the roof is only one component of the building's sensible cooling heat load, so the percentage increase in cooling energy consumption will be less than the percentage increase in roof heat flow.

For brevity, “effective thermal conductivity” will be referred to simply as “conductivity” in the remainder of this paper.

Equipped with a special function to examine attic heat transfer (Gartland & Akbari 1996), the DOE-2 building energy model was used to study the effect of the temperature-dependent conductivity on cooling energy load. First, the specially-equipped energy model was applied to a school bungalow whose surface temperature and cooling energy consumption had been measured in a 1992 investigation of the effect of roof albedo on cooling energy use (Akbari et al. 1993). Hourly values of roof heat flux, surface temperature and cooling power were simulated with and without variable conductivity. Temperatures and cooling powers were then

compared to measured values to determine whether incorporation of the temperature dependence of conductivity made the DOE-2 model more accurate.

Next, the effect of variable conductivity on cooling energy consumption was simulated for various climates. The annual cooling energy load and annual peak hourly cooling power demand of a typical, medium-sized office building was simulated first with nominal and then with variable conductivity in five different climates.

**School Bungalow Experiment.** The first building modeled was an air-conditioned school bungalow in Sacramento, Calif., that had been monitored in the summer and fall of 1992. This one-room,  $89\text{ m}^2$  structure had R-11 walls, two-pane windows, and a corrugated metal roof insulated with six-inch thick, R-19 fiberglass. It was vacant in August because school was not in session; it was reoccupied on September 8 when classes resumed.

The metal roof was painted brown for the month of August, and repainted white for the month of September. When brown, the roof absorbed 92% of incident sunshine, heating its surface to a peak measured daytime temperature of  $72^\circ\text{C}$  (Figure 2). When white, the roof absorbed only 32% of incident sunshine, and its peak daytime surface temperature was measured to be  $35^\circ\text{C}$  (Figure 3). Since the air temperature inside the building was maintained at  $26^\circ\text{C}$  from 9 am to 7 pm, the insulation reached a peak mean temperature of approximately  $49^\circ\text{C}$  beneath the brown roof, but only  $31^\circ\text{C}$  beneath the white roof. Thus the brown roof was “hot”, and the white roof was “cool”.

The components of the building's sensible cooling heat load are listed in Table 1.

**Figure 2.** Brown (Hot) Roof Surface Temperature vs. Time of Day

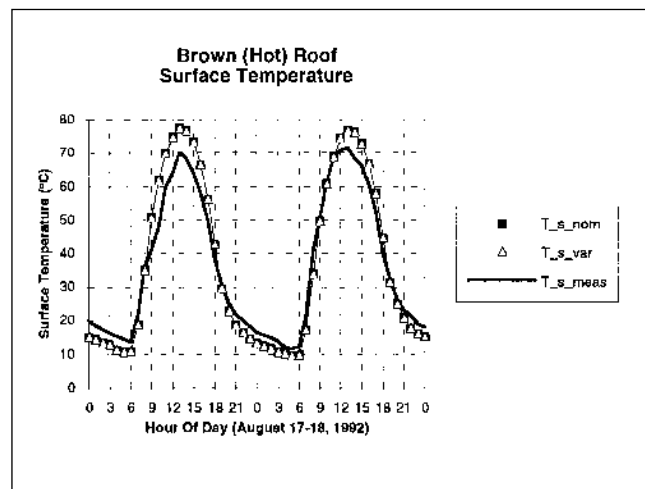


**Figure 3.** White (Cool) Roof Surface Temperature vs. Time of Day

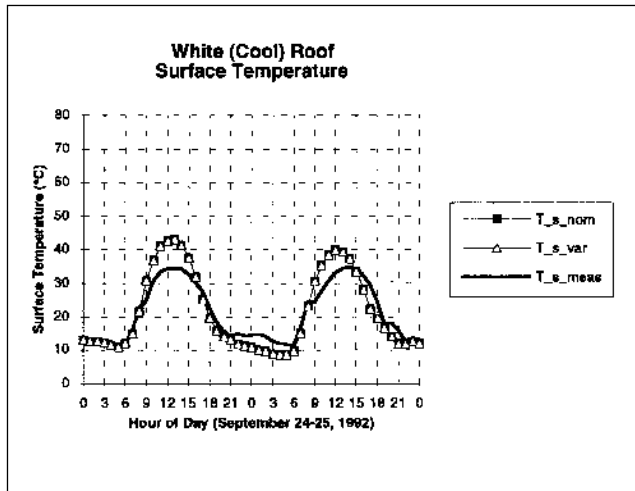


**Table 1.** Breakdown of School Bungalow's Sensible Cooling Heat Load by Component

	Brown (Hot) Roof	White (Cool) Roof
Room:		
Internal	0%	45%
Shell	100%	55%
Shell:		
Roof	43%	20%
Walls	27%	36%
Windows	19%	30%
Infiltration	11%	13%
Roof Component of Building Load	43%	11%

The nominal R-value of the six-inch fiberglass roof insulation was 19 ( $R_{nom} = 19 \text{ hr ft}^2 \text{ }^\circ\text{F BTU}^{-1}$ ) at  $T_{room} = 21^\circ\text{C}$ , yielding a nominal effective thermal conductivity of 0.32 BTU in  $\text{hr}^{-1} \text{ ft}^{-2} \text{ }^\circ\text{F}^{-1}$ , or  $0.046 \text{ W m}^{-1} \text{ K}^{-1}$ . In Figure 1,  $k_e(T_{room}) \approx 0.046 \text{ W m}^{-1} \text{ K}^{-1}$  for fiberglass of density  $\rho = 12 \text{ kg m}^{-3}$ . Over the range of mean temperatures experienced by insulation in this building's attic—say  $21^\circ$  to  $50^\circ\text{C}$ —the curve  $k_e(T)_{\rho=12}$  is reasonably well approximated by

$$k_e(T) = k_{e_{nom}} [1 + c (T - T_{room})],$$

where  $c = 0.00752 \text{ }^\circ\text{C}^{-1}$  and  $T$  is in degrees Celsius. The thermal conductivity predicted by this function is 22% higher at  $50^\circ\text{C}$  than at room temperature.

In the calculations below, the subscripts *nom* and *var* denote values computed using nominal and variable conductivities, respectively. The percentage increase in a quantity  $x$  due to the effect of variable conductivity is denoted  $x_{rel}$ , and is defined as

$$x_{rel} = \frac{x_{var} - x_{nom}}{x_{nom}} \times 100\%.$$

The roof insulation mean temperature  $T_m$  is given approximately by

$$T_m \approx \frac{1}{2} (T_s + T_i),$$

where  $T_s$  is the roof surface temperate and  $T_i$  is the inside air temperature.

For each roof,  $x_{nom}$ ,  $x_{var}$ , and  $x_{rel}$  were calculated for the following quantities  $x$ :

- (1) hourly surface temperature  $T_s$  ( $^\circ\text{C}$ );
- (2) hourly roof heat flux  $q$  (kW);
- (3) hourly heat-pump cooling power  $e$  (kW);
- (4) roof component of monthly sensible cooling heat load,  $Q$  (kWh); and
- (5) monthly heat-pump cooling energy consumption,  $E$  (kWh).

**Five Climates.** The annual cooling energy load and annual peak hourly cooling power load were computed with and without variable thermal conductivity for a medium-sized office building.

This five-zone, single-story,  $2,840 \text{ m}^2$  structure has a brown roof, six-inch-thick R-19 fiberglass insulation, R-7 walls, and single-pane windows. Simulations were run for five climates:

- (1) Lake Charles, Louis.—warm winter, hot and humid summer;
- (2) Minneapolis, Minn.—very cold winter, mild summer;
- (3) Phoenix, Ariz.—hot and dry year-round;
- (4) Sacramento, Calif.—warm winter, warm summer; and
- (5) Washington, D.C. —cold winter, warm summer.

The variable conductivity function  $k_e(T)$  used for the school bungalow was also used for the office building.

## RESULTS

### School Bungalow Experiment

For the brown roof, variable thermal conductivity had a negligible effect on roof surface temperature ( $-1\% < T_{s,rel} < 0\%$ ), a strong effect on roof heat flows ( $-4\% < q_{rel} < 21\%$ ), and a moderate effect on cooling power ( $0\% < e_{rel} < 10\%$ ) (Figure 4). For the white roof, variable thermal had a negligible effect on roof surface temperature ( $-1\% < T_{s,rel} < 0\%$ ), a moderate effect on roof heat flow ( $-4\% < q_{rel} < 8\%$ ), and a negligible effect on cooling power ( $0\% < e_{rel} < 1\%$ ) (Figure 5).

**Hourly Surface Temperature.** The high thermal resistance of the roof made conduction through the roof relatively unimportant in the energy balance that determined the roof surface temperature. If the brown roof absorbs  $900 \text{ W m}^{-2}$  of insolation and achieves a surface temperature of  $80^\circ\text{C}$ , only  $16 \text{ W m}^{-2}$ , or 2%, will be conducted through its R-19 insulation to the  $26^\circ\text{C}$  inside air. Similarly, if the white roof absorbs  $300 \text{ W m}^{-2}$  of insolation and reaches  $35^\circ\text{C}$ , it will conduct only  $3 \text{ W m}^{-2}$ , or 1%, through the roof. Increasing this small flow by 20% has little effect on the energy balance, so we find  $T_{var} \approx T_{nom}$ .

Simulated temperatures were generally higher than measured temperatures (Figures 2 and 3), primarily because the external convection coefficient used in this DOE-2 simulation was chosen to make the predicted cooling power load

**Figure 4.** Brown (Hot) Roof Surface Temperature, Roof Heat Flow, and Cooling Power Increases Due to Variable Thermal Conductivity vs. Time of Day

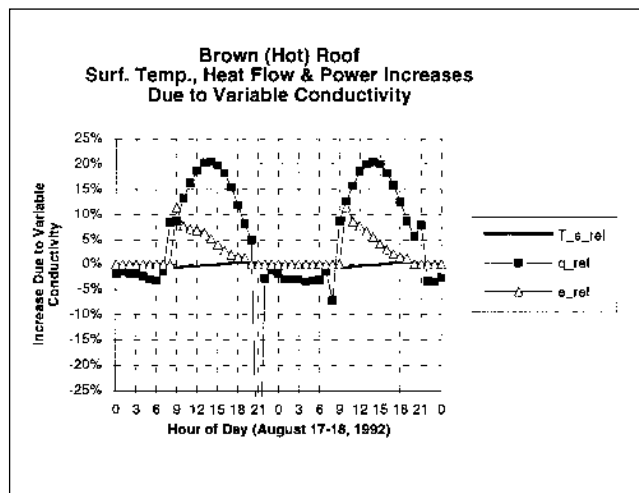
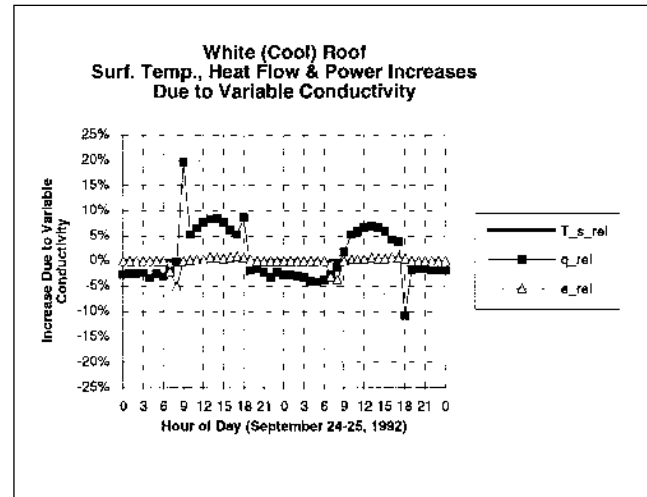


**Figure 5.** White (Cool) Roof Surface Temperature, Roof Heat Flow, and Cooling Power Increases Due to Variable Thermal Conductivity vs. Time of Day



match the measured cooling power load, rather than to make the predicted surface temperature match the measured surface temperature (Gartland & Akbari 1996).

**Hourly Roof Heat Flow.** The simulated roof heat flow behaved as expected: variable conductivity made the heat flow increase during the day, when  $T_m > 21^\circ\text{C}$ , and decrease at night, when  $T_m < 21^\circ\text{C}$  (Figures 6 and 7). Plotting  $q_{rel}$  versus  $q_{nom}$  suggests that the temperature variation of R-value tends to make buildings warmer in summer by increasing the daily inward roof heat flux and decreasing the nightly outward roof heat flux (Figure 8).

A little analysis shows that the percent increase in roof heat flow should be approximately equal to the percentage rise

**Figure 6.** Brown (Hot) Roof Heat Flow vs. Time of Day

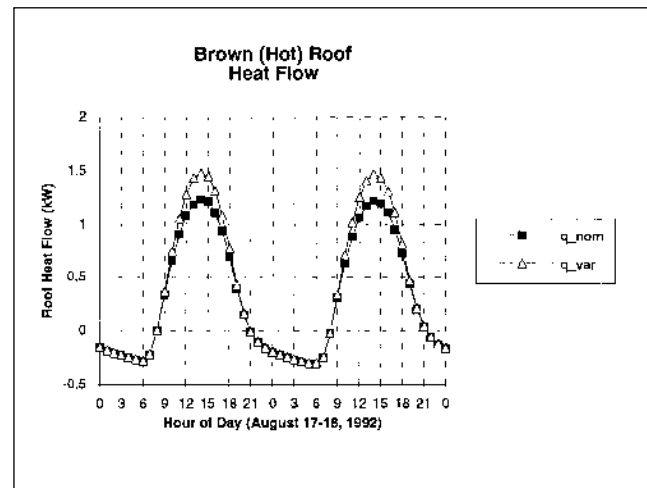


**Figure 7. White (Cool) Roof Heat Flow vs. Time of Day**

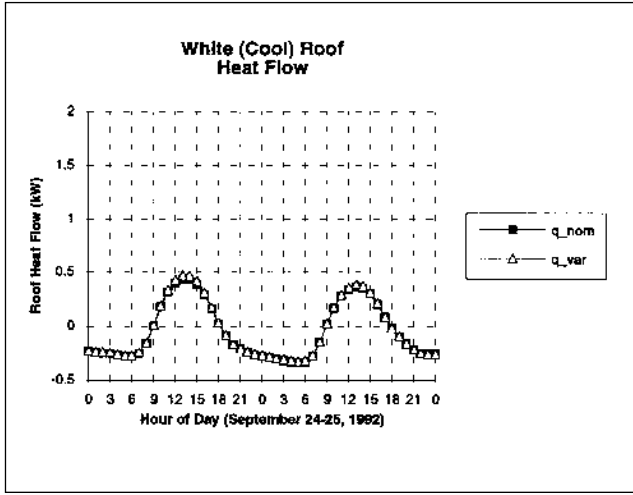
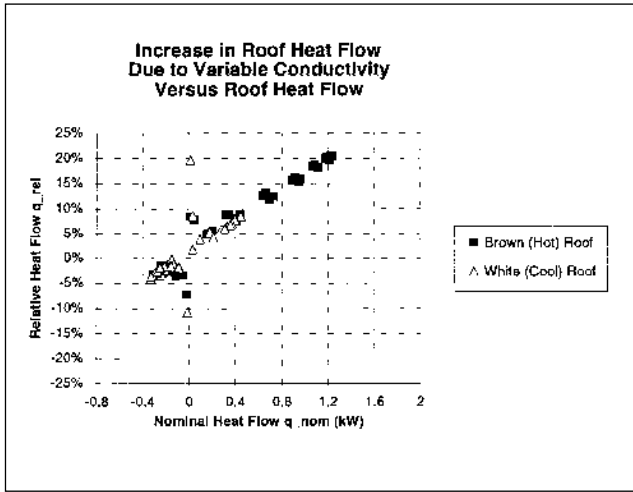


**Figure 8. Increase in Roof Heat Flow Due to Variable Thermal Conductivity, vs. Roof Heat Flow**



in thermal conductivity. Applying Fourier's law to the temperature difference across the insulation,

$$q_{nom} = -k_e \frac{dT}{dx} \approx k_{e_{nom}} [T_s - T_i]/l$$

and

$$q_{var} = -k_e \frac{dT}{dx} \approx k_{e_{var}} [T_s - T_i]/l$$

Noting that  $T_i$  is held constant during the day, and that  $T_s$  is insensitive to variable thermal conductivity,

$$q_{rel} \approx k_{e_{rel}}.$$

Simulation of the brown roof predicted a peak  $T_s = 77^\circ\text{C}$ , and thus a peak  $T_m = 52^\circ\text{C}$ ; this yields  $q_{rel} \approx k_{e_{rel}}$

$(52^\circ\text{C}) = 21\%$ . For the white roof, peak values were  $T_s = 43^\circ\text{C}$  and  $T_m = 35^\circ\text{C}$ , yielding  $q_{rel} \approx k_{e_{rel}} (35^\circ\text{C}) = 10\%$ . These are close to the peak  $q_{rel}$  of 21% and 8% observed for the brown and white roofs.

**Hourly Cooling Power.** In the case of the white, cool roof, small values of  $q_{rel}$  ( $q_{rel} < 8\%$ ), combined with the small contribution of roof to the total sensible cooling heat load—roof load was 20% of the shell load, which in turn was 55% of total load; thus roof load was 11% of the total load—made the cooling power (Figure 9) insensitive to the temperature variation of thermal conductivity.  $e_{rel}$  was less than 1% (Figure 5).

In the case of the brown roof, the roof contributed 43% of the total heat load, so we would expect  $e_{rel}$  to be approximately 43% of  $q_{rel}$  when the air conditioning was on. That is,  $e_{rel} \approx 0.43 q_{rel}$  should be 4% at 9 am, 10% at 1 pm, and 2% at 7 pm. Instead, we find  $e_{rel}$  is 10% at 9 am, 6% at 1 pm, and 0% at 7 pm (Figure 4). This may be due in part to additional roof heat flow at 8 am, when  $q_{rel} = 10\%$ , which heats the building before the air conditioning turns on at 9 am. This would increase the cooling load at the start of the around 9 am. However, the behavior of  $e_{rel}$  over the rest of the day remains somewhat puzzling.

Comparing  $e_{nom}$  and  $e_{var}$  to  $e_{meas}$ , we can see that  $e_{var}$  was appreciably closer to  $e_{meas}$  than was  $e_{nom}$  between 9 am and 3 pm, and slightly further away between 3 pm and 7 pm (Figure 10). The total deviation of  $e_{var}$  from  $e_{meas}$  was 15% smaller than that of  $e_{nom}$ . Here the deviation has been computed as

**Figure 9. White (Cool) Roof Cooling Power Consumption vs. Time of Day**

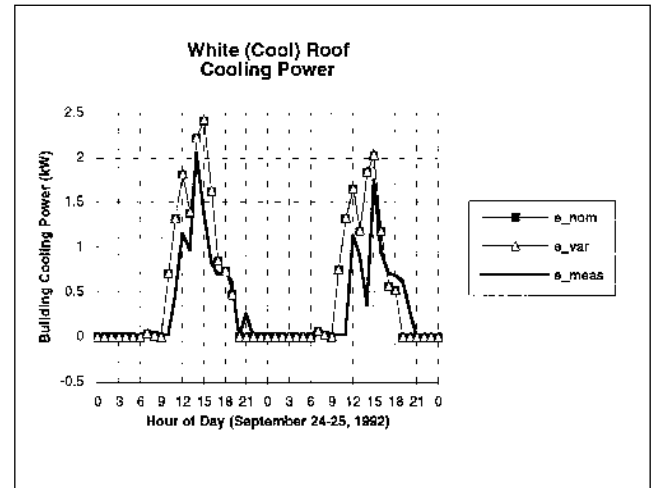


**Figure 10.** Brown (Hot) Roof Cooling Power Consumption vs. Time of Day

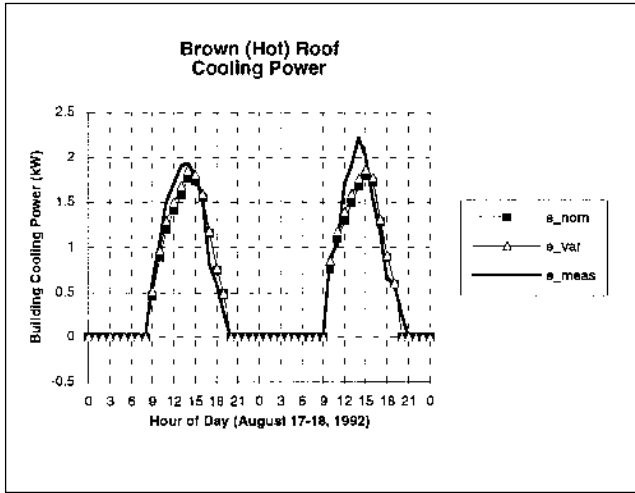
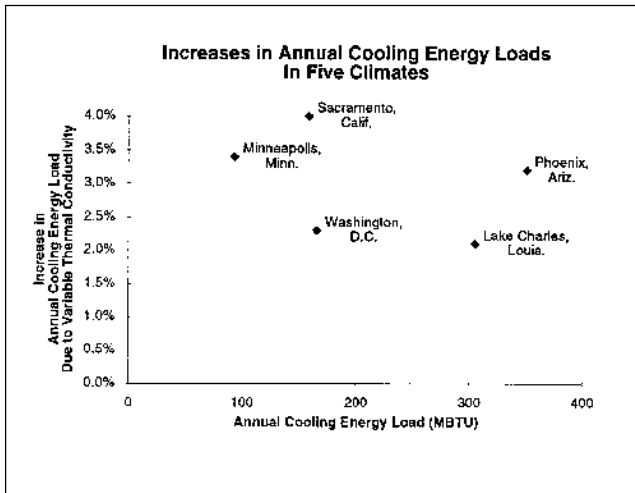


**Figure 11.** Increase in Annual Cooling Energy Load of an Office Building vs. Annual Cooling Energy Load, Simulated for Five Climates



$$\sqrt{\frac{\sum_{j=1}^J (e_{\text{simulated}_j} - e_{\text{meas}_j})^2}{J}}$$

where  $J$  is the number of data points.

**Roof Component of Monthly Sensible Cooling Heat Load.** Variable conductivity increased the brown roof's  $Q$  by 22% during the month of August, and increased that of the white roof by 8%. These are a little higher than expected, since the peak values of  $q_{\text{rel}}$  observed in Figures 4 and 5 were 21% and 8% for the brown and white roofs, respectively.

**Monthly Heat-Pump Cooling Energy Consumption.** Variable conductivity increased the cooling energy  $E$  drawn by the building heat's pump by 8% in August (for the brown roof) and 0.5% in September (for the white roof).  $E_{\text{rel}}$  was much greater for the brown roof than the white roof because both  $Q_{\text{rel}}$  and the roof percentage of the sensible cooling heat load were higher for the brown roof than for the white roof. For the brown roof, the roof load was 43% of the total load, so we expect  $E_{\text{rel}} = 0.43 Q_{\text{rel}} = 0.43 (22\%) = 9.5\%$ ; for the white roof, the roof load was 11% of the total load, so we expect  $E_{\text{rel}} = 0.11 Q_{\text{rel}} = 0.11 (8\%) = 0.9\%$ . These values are close to the predicted  $E_{\text{rel}}$  of 8% and 0.5%.

## Five Climates

The annual cooling energy load and annual peak hourly cooling power load of the medium-sized office building are shown in Table 2. The breakdown of the building's sensible cooling heat load by component is given in Table 3.

The introduction of variable thermal conductivity increased annual cooling energy loads by 2% to 4%. One would expect to the cities with the warmest climates to show the greatest percentage increase in annual cooling energy loads. However, this was not found to be the case: plotting the percentage increase versus the annual energy load reveals no particular pattern (Figure 11). The reason for this is not clear.

## CONCLUSIONS

The temperature dependence of the effective thermal conductivity of fiberglass insulation led to moderate increases in the simulated cooling energy load of a typical office building. Simulations of the school bungalow suggest that variable conductivity yields the greatest increase in cooling energy consumption when (a) the roof is dark, leading to a high daytime surface temperature; and (b) heat flow through the roof accounts for a large fraction of the building's sensible cooling heat load. Buildings with highly-reflective roofs, large internal heat loads, or large heat loads through parts of the shell other than the roof will be less sensitive to temperature variations in conductivity.

Incorporating variable conductivity into the DOE-2 building energy model brought simulated values of the school bungalow's cooling power 15% closer to those measured in the monitoring experiment. Simulations of other monitored buildings will be needed to determine the generality of this result.

## ACKNOWLEDGMENTS

This work was supported by the Assistant Secretary for Conservation and Renewable Energy, Office of Building

**Table 2.** *Climate Simulation of the Annual Cooling Energy Load and Annual Peak Hourly Cooling Power Load of a Typical Office Building*

Location	Thermal Conductivity	Annual Cooling Energy Load (MBTU)	Annual Peak Hourly Cooling Power (kW)	Peak Time
Lake Charles, Louis.	nominal k	305.3	153.2	noon, Aug 2
	variable k	311.6	154.3	noon, Aug 2
	change	+ 2%	+ 1%	
Minneapolis, Minn.	nominal k	93.3	139.4	4 pm, Aug 2
	variable k	96.5	141.7	4 pm, Aug 2
	change	+ 3%	+ 2%	
Phoenix, Ariz.	nominal k	350.8	162.0	4 pm, Aug 2
	variable k	362.1	164.4	4 pm, Aug 2
	change	+ 3%	+ 1%	
Sacramento, Calif.	nominal k	158.8	149.4	4 pm, July 12
	variable k	165.1	152.4	4 pm, July 12
	change	+ 4%	+ 2%	
Washington, D.C.	nominal k	166.1	140.8	4 pm, July 23
	variable k	170.0	142.6	4 pm, July 23
	change	+ 2%	+ 1%	

Note: “change” refers to the increase in cooling energy load or power due when nominal thermal conductivity is replaced by variable thermal conductivity.

**Table 3.** *Breakdown of Office Building’s Sensible Cooling Heat Load by Component*

	Lake Charles, Louis.	Minneapolis, Minn.	Phoenix, Ariz.	Sacramento, Calif.	Washington, D.C.
Building:					
Internal	74%	77%	63%	72%	78%
Shell	26%	23%	37%	28%	22%
Shell:					
Roof	45%	39%	40%	41%	40%
Other	55%	61%	60%	59%	60%
Roof Component of Building Load	12%	9%	15%	11%	9%

Technologies of the U. S. Department of Energy, under contract No. DE-AC0376SF00098.

## REFERENCES

- Akbari, H., S.E. Bretz, J.W. Hanford, D.M. Kurn, B.L. Fishman, H.G. Taha, and W. Bos. 1993. *Monitoring Peak Power and Cooling Energy Savings of Shade Trees and White Surfaces in the Sacramento Municipal Utility District (SMUD) Service Area: Data Analysis, Simulations and Results*. LBL-34411. Berkeley, Cal: Lawrence Berkeley Laboratory.
- American Society of Heating, Refrigerating, and Air-Conditioning Engineers. 1985. *ASHRAE Handbook of Fundamentals, IP ed.* Atlanta, GA: American Society of Heating, Refrigerating, and Air-Conditioning Engineers.
- Brewster, M.Q. 1992. *Thermal Radiative Transfer and Properties*. Wiley.
- Cabannes, F., J-C Maurau, M. Hyrien, S.M. Klarsfeld. 1979. "Radiative Heat Transfer in Fibreglass Insulating Materials as Related to Their Optical Properties." *High Temperatures - High Pressures* 11:429-434.
- Gartland, L. and H. Akbari. ACEEE paper #94, LBL-38580.
- Gebhart, B. 1993. *Heat Conduction and Mass Diffusion*. McGraw-Hill.
- Kaviany, M. 1991. *Principles of Heat Transfer in Porous Media*. Springer-Verlag.
- Powell, F., M. Krarti, and A. Tuluca. 1989. "Air Movement Influence on the Effective Thermal Resistance of Porous Insulations: A Literature Survey." *Journal of Thermal Insulation* 12:239-250.
- Pratt, A.W. 1969. "Heat Transmission in Low Conductivity Materials." *Thermal Conductivity vol. 1. edited by R.P. Tye*. Academic Press.
- Progelhof, R.C., J.L Throne, and R.R. Ruetsch. 1976. "Methods for Predicting the Thermal Conductivity of Composite Systems: A Review." *Polymer Engineering and Science* 16 (9):615-625.
- Tong, T.W. and C.L. Tien. 1983. "Radiative Heat Transfer in Fibrous Insulations - Part I: Analytical Study & Part II: Experimental Study." *Journal of Heat Transfer* 105 (1):70-81.
- Turner, W.C. and J.F. Malloy. 1981. *Thermal Insulation Handbook*. McGraw-Hall.
- White, F. 1988. *Heat and Mass Transfer*. Addison-Wesley.
- Wilkes, K. 1981. "Thermophysical Properties Data Base Activities at Owens-Corning Fiberglass". In *Proceedings of the ASHRAE/DOE-ORNL Conference "Thermal Performance of the Exterior Envelope of Buildings"*, 662-77. ASHRAE SP 28.